Formation control of stochastic multi-vehicle systems

Violet Mwaffo*, *Member, IEEE,* Pietro DeLellis, *Member, IEEE,* Sean Humbert

***Abstract*—In this paper, we propose a decentralized approach to formation control in groups of stochastic mobile robots. Different from existing work, we explicitly model the presence of stochastic perturbations affecting the dynamics, and model the multi-vehicle system through stochastic differential equations. We design a decentralized formation control strategy where only a subset of informed agents is aware of the desired target locations, and derive sufficient conditions for almost sure convergence to the desired formation pattern. Specifically, we illustrate how the achievement of the control goal is related to the intensity of the noise and to the topology of the communication graph among the robots. The proposed formation control strategy is tested through extensive numerical analyses and validated experimentally on ground robots.**

***Index Terms*—Autonomous systems, formation control, non-holonomic unicycle models, stochastic systems, swarm robotics.**

I. Introduction

The spontaneous emergence of collective behaviors in animal groups [1]–[3], as well as in biological and social networks [4], [5], has inspired the design of several engineering systems and notably swarms of mobile robots and unmanned undersea or aerial vehicles [6]–[12]. In animal groups, coordinated behavior originates from local interaction between individuals, and provides several benefits to the entire group, such as a more efficient foraging or a more effective defense against predators [1]–[3]. Similarly, in robotic swarms, coordinated motion is useful to perform complex tasks that might not be achieved by a single unit [11], [13], [14], as for instance collective search and rescue missions over off-road rough terrains and large areas, or collective transportation of multiples units or large-sized objects [15]. Inspired by examples from the animal kingdom, coordination in swarm robotic systems is achieved by allowing individuals in the group to communicate and cooperate toward the achievement of a common goal, as for instance aggregation, cohesion, or the achievement of a desired formation [9], [11], [14], [16].

A widely studied problem in the area of multi-agent systems is formation control, where a group of autonomous vehicles is required to track a predefined path or trajectory while keeping a prescribed spatial configuration [17]–[21]. With the recent progress in electronics, sensor integration, and 3D printing fabrication resulting in a significant reduction in component prices and allowing rapid prototyping, autonomous vehicles and robots have become accessible not only for military but also civil applications [22]–[24]. In swarm robotics, leader-followers control schemes have been developed to efficiently control the group of robots or drones. Specifically, a single or few leaders are equipped with advanced and expensive navigation sensors to drive the rest of the group (the followers) equipped with less accurate, but cheaper proximity sensors [16], [25]–[28].

Group coordination in leader-follower systems has been intensively investigated in the literature of multi-agent systems [18] by employing both numerical simulations [29], [30] and analytical methods [31]–[35], which then have been experimentally validated [36]. Research efforts on formation control schemes have addressed the problem of achieving a desired formation, tracking a trajectory identified by an informed leader [37], [38], and adapting to environmental constraints by avoiding obstacles and collisions [36]. The problem of achieving a desired formation in a three-dimensional space while guaranteeing that minimal safety distances are maintained has been tackled in [39], [40]. When motion in a two-dimensional space is considered, as in the case of swarms of ground robots, the individual agent is often

Manuscript received May 28, 2020

This work was supported by the Chancellor Postdoctoral Fellowship, the Autonomous System IRT Seed Grant, the Summer Program for Undergraduate Research of the University of Colorado Boulder; and by the program "STAR 2018" of the University of Naples Federico II and Compagnia di San Paolo, Istituto Banco di Napoli - Fondazione, project ACROSS.

V. Mwaffo was with the Department of Mechanical Engineering, University of Colorado, Boulder, CO, USA (e-mail: violet.mwaffo@colorado.edu). He is now with the Weapons, Robotics, and Control Engineering Department, United States Naval Academy, Annapolis, MD 21402 USA (e-mail: mwaffo@usna.edu).

P. DeLellis is with the Department of Electrical Engineering and Information Technology, University of Naples Federico II, Naples, Italy (e-mail: pietro.delellis@unina.it).

S. Humbert is with the Department of Mechanical Engineering, University of Colorado, Boulder, CO, USA (e-mail: sean.humbert@colorado.edu).

*Corresponding author: violet.mwaffo@colorado.edu.

modeled as a non-holonomic unicycle vehicle [41]–[45]. This model is widely used in applications [46], and has proved to be particularly suitable for robots with one castor, two differentially driven wheels [41], or 2-D motion of fixed wind aircrafts [47].

In formation control problems, the effect of noise on the actuation force and control torque was seldom considered in the literature. However, in real world systems, non-holonomic robots might be subject to perturbations due to internal factors such as fluctuations of the power supply, possible component failures, chassis vibrations, or environmental factors such as off-road rough terrain, wind gusts, and sensor measurement errors [48]. These intermittent and unpredictable perturbations can be suitably modeled as stochastic noise [49], [50], but their effect has been studied so far only on first order non-holonomic unicycle models [47], [48], [51]. In these works, numerical methods have been proposed to solve an optimal feedback control problem, but the robustness of the control strategy to the magnitude of the noise has not been explored. In different contexts, the robustness to noise has been explored [52]–[54], with a focus on control of manipulators [53] and of multi-agent quadrotor systems [54]. To the best of our knowledge, no previous work has studied the impact of noise on the second order non-holonomic unicycle model, which is indeed a more suitable framework [41] to study 2-D motion of ground robots or fixed-wing aircraft [37], [41].

In this manuscript, we devise a leader-follower cooperative control strategy for formation control in groups of planar non-holonomic unicycle mobile robots, that is capable of coping with possible uncertainties on the actuation force and control torque. In particular, by combining the stability theory for stochastic differential equations with graph-theoretic tools, we provide sufficient conditions for almost sure convergence of the formation towards the desired locations. Our analytical conditions put in evidence the interplay between the properties of the network topology, the individual dynamics of the robots, and the intensity of the noise. The proposed decentralized control strategy is then tested numerically, and its robustness to increasing noise on both the input force and torque is investigated through extensive simulations. Finally, we perform experiments on ground robots that i) validate our modeling approach and ii) show that our theoretical conditions can be used to enforce convergence in the presence of a slippery terrain.

The rest of the paper is organized as follows. The mathematical preliminaries on stochastic differential equations and graph theory are provided in Section II. In Section III, the robotic model is introduced and the formation control problem is formulated. The proposed decentralized leader-follower control strategy is presented in Section IV, together with the main results on the almost sure convergence towards the desired formation. The numerical analysis is articulated in Section V, while the experimental results are discussed in Section VI. Finally, conclusions are drawn in Section VII.

II. Mathematical Preliminaries

A. Notation

Throughout the manuscript, I_m denotes the identity matrix of size m, $0_{m\times p}$ the $m \times p$ matrix with all zero elements, and $\|v\|_2$ the Euclidean norm of a vector v. Given a real matrix M, we denote by $\|M\|_* = \sqrt{\mathrm{trace}\,(M^T M)}$ its nuclear norm. When $M = M^T \in \mathbb{R}^{m\times m}$, we sort its real eigenvalues in ascending order as $\lambda_1(M) \leq \ldots \leq \lambda_m(M)$. Given $A, B \subseteq \mathbb{R}$, we denote by $L^1(A, B)$ the space of Lebesgue integrable functions $\rho : A \to B$. Also, we introduce the family $C^{2,1}\left(\mathbb{R}^n \times \mathbb{R}^+, \mathbb{R}^+\right)$ of nonnegative functions $V(x,t)$ on $\mathbb{R}^n \times \mathbb{R}^+$ that are continuously twice differentiable in x, and an operator $\mathcal{L}$ acting on $C^{2,1}\left(\mathbb{R}^n \times \mathbb{R}^+, \mathbb{R}^+\right)$ functions and defined as

$$\begin{aligned}\mathcal{L}V(x,t) =& \frac{\partial V(x,t)}{\partial t} + \frac{\partial V(x,t)}{\partial x} f(x,t) \\ &+ \frac{1}{2}\mathrm{trace}\left(g^T(x,t)\frac{\partial^2 V(x,t)}{\partial x^2} g(x,t)\right),\end{aligned}$$

where $f : \mathbb{R}^n \times \mathbb{R}^+ \to \mathbb{R}^n$, $g : \mathbb{R}^n \times \mathbb{R}^+ \to \mathbb{R}^{n\times m}$ are real functions,

$$\frac{\partial V(x,t)}{\partial x} = \left[\frac{\partial V(x,t)}{\partial x_1}, ..., \frac{\partial V(x,t)}{\partial x_n}\right]$$

and

$$\left[\frac{\partial^2 V(x,t)}{\partial x^2}\right]_{ij} = \left[\frac{\partial^2 V(x,t)}{\partial x_i \partial x_j}\right],$$

for all $i, j = 1, \ldots, n$.

B. Stochastic systems

Let $\mathcal{P} = \{\Gamma, F, P\}$ be a complete probability space with filtration $\{F\}_{t\geq 0}$, where Γ is the sample space, F is a σ-algebra of measurable subsets of Γ, and $P : F \to [0, 1]$ is a probability measure. The filtration $\{F\}_{t\geq 0}$ is right-continuous and contains all P-null sets, i.e. sets of events with zero probability of occurrence. Next, we introduce the non-autonomous n-dimensional stochastic system

$$\mathrm{d}x(t) = f(x(t), t)\mathrm{d}t + g(x(t), t)\mathrm{d}W(t), \qquad (1)$$

with initial condition $x(0) = x_0$, where $x(t) \in \mathbb{R}^n$ is the state of the system at time $t \geq 0$, $W(t) =$

$[W_1(t), \dots, W_m(t)]^T$ is an m-dimensional Wiener process [55] defined on $\mathcal{P}$, and f and g are measurable functions verifying:

Assumption II.1. *f and g satisfy the generalized Lipschitz condition, that is, for all $j = 1, 2, \dots$, there exists $c_j > 0$ such that,*

$$\begin{aligned} \|f(x,t) - f(y,t)\|_2 &\leq c_j \|x - y\|_2 , \\ \|g(x,t) - g(y,t)\|_* &\leq c_j \|x - y\|_2 , \end{aligned} \tag{2}$$

for all $t \geq 0$, and $x, y \in \mathbb{R}^n$ such that $\|x\|, \|y\| \leq j$. Furthermore, f and g also satisfy the linear growth condition, that is, there exists $c > 0$ such that

$$\begin{aligned} \|f(x,t)\|_2 &\leq c\,(1 + \|x\|_2) , \\ \|g(x,t)\|_* &\leq c\,(1 + \|x\|_2) , \end{aligned} \tag{3}$$

for all $x \in \mathbb{R}^n$.

When the above assumption holds, system (1) has a unique continuous solution [56, Cor. 6.3.1], [57, Ch. 5, Thm 1.1], [58] say $x(t, x_0)$, for $t \geq 0$ and, moreover, for all $p > 0$, we have

$$\mathbf{E}\left[\sup_{0 \leq \tau \leq t} \|x(\tau, x_0)\|_2^p\right] < +\infty, \qquad \text{for } t \geq 0.$$

If there exists a P-null set $\Gamma_0 \in \mathcal{F}$ such that for every $\gamma \notin \Gamma_0$, the sequence $x(t, x_0)$ converges to $\bar{x}$ in the usual sense in $\mathbb{R}^n$, then $x(t, x_0)$ is said to converge to $\bar{x}$ almost surely (or with probability 1), and we write

$$\lim_{t \to +\infty} x(t, x_0) = \bar{x} \text{ a.s.}$$

We can now give the following Lemma, which is a stochastic version of the LaSalle theorem that allows to characterize the asymptotic behavior of the stochastic system (1) in a probabilistic sense:

Lemma II.2. *[58] If*

1) *Assumption II.1 holds;*
2) *g is bounded;*
3) *There exist a function $V \in C^{2,1}(\mathbb{R}^n \times \mathbb{R}^+, \mathbb{R}^+)$, and a continuous function $\mu : \mathbb{R}^n \to \mathbb{R}^+$ such that*

$$\lim_{\|x\|_2 \to +\infty} \inf_{t \in \mathbb{R}^+} V(x,t) = +\infty, \tag{4a}$$

$$\mathcal{L}V(x,t) \leq -\mu(x), \quad (x,t) \in \mathbb{R}^n \times \mathbb{R}^+. \tag{4b}$$

Then, for every $x_0 \in \mathbb{R}^n$,

- $\lim_{t \to +\infty} V(x(t, x_0), t)$ *exists and is finite almost surely;*
- $\lim_{t \to +\infty} \mu(x(t, x_0)) = 0$ *almost surely.*

Finally, we provide the Itô's formula, which will be used to perform the computations throughout the manuscript.

Lemma II.3. *[59] Let us consider a function $V \in C^{2,1}(\mathbb{R}^n \times \mathbb{R}^+, \mathbb{R})$. Then, $V(x(t), t)$ is an Itô process with the stochastic differential given by*

$$\begin{aligned} \mathrm{d}V(x(t),t) = \Bigg(&\frac{\partial V(x(t),t)}{\partial t} + \frac{\partial V(x(t),t)}{\partial x} f(x,t) + \\ &+ \mathrm{trace}\left(g^T(x,t) \frac{\partial^2 V(x(t),t)}{\partial x^2} \right) g(x,t) \Bigg) \mathrm{d}t \\ &+ \frac{\partial V(x(t),t)}{\partial x} g(x,t) \mathrm{d}W(t) \quad \text{a.s.} \end{aligned} \tag{5}$$

C. Graphs

Let $\mathcal{G} = \{\mathcal{V}, \mathcal{E}, \mathcal{W}\}$ be an undirected connected graph, where $\mathcal{V} = \{1, \dots, N\}$ is the set of nodes, $\mathcal{E} \subseteq \mathcal{V} \times \mathcal{V}$ is the set of edges, and $\mathcal{W}$ is the set of scalar weights $w_{ij} = w_{ji}$, $(i,j) \in \mathcal{E}$. The graph topology can be described by the binary adjacency matrix A, whose generic element a_{ij} is one if $(i,j) \in \mathcal{E}$, while it is zero otherwise. An alternative description of the graph, which will be useful in the following, is through the weighted Laplacian matrix $L \in \mathbb{R}^{N \times N}$, whose element L_{ij} is defined as

$$L_{ij} = \begin{cases} -a_{ij} w_{ij}, & \text{if } (i,j) \in \mathcal{E}, \\ 0, & \text{if } (i,j) \notin \mathcal{E}, i \neq j, \\ \displaystyle\sum_{j=1, j \neq i}^{N} a_{ij} w_{ij}, & \text{if } i = j. \end{cases} \tag{6}$$

From its definition, matrix L has zero row-sums, that is, $\sum_{j=1}^N L_{ij} = 0$, for all $i = 1, \dots, N$. Furthermore, being the graph connected and undirected, it is an irreducible matrix, $\mathrm{rank}(L) = N - 1$, and all its eigenvalues are real and can be sorted in ascending order as $0 = \lambda_1(L) < \lambda_2(L) \leq \dots \leq \lambda_N(L)$ [60].

Lemma II.4. *[61]. Let M be an m-dimensional irreducible square matrix whose ij-th element is denoted by m_{ij}, and let D be a diagonal matrix $D := \mathrm{diag}(D_1, \dots, D_m)$, with $D_i \geq 0$ for all i, and $\sum_{i=1}^m D_i > 0$. If $\mathrm{rank}(M) = m - 1$, $m_{ij} = m_{ji} \leq 0$ for all $i \neq j$, and $\sum_{j=1}^m m_{ij} = 0$ for all i, then the eigenvalues of the matrix $Z := M + D$ are all real and positive.*

From the above Lemma, it follows that if we sum to an irreducible weighted graph Laplacian L, associated to a connected undirected graph, a nonnegative diagonal matrix D with at least one positive element, then all the eigenvalues of $L + D$ are real and strictly positive.

III. Problem Statement

A. Robotic model

In this paper, we consider the problem of coordinating the motion of a group of N mobile planar robots coupled through an undirected connected graph $\mathcal{G} = \{\mathcal{V}, \mathcal{E}, \mathcal{W}\}$, where $\mathcal{V} = \{1, \dots, N\}$ is the set of nodes representing the robots, $\mathcal{E}$ is the set of edges that connect interacting robots, and $\mathcal{W}$ is the set of weights quantifying the intensity of the coupling among connected robots. The individual dynamics is described by the following stochastic non-holonomic unicycle model:

$$\mathrm{d}x_i(t) = v_i(t)\cos\left(\theta_i(t)\right)\mathrm{d}t, \tag{7a}$$

$$\mathrm{d}y_i(t) = v_i(t)\sin\left(\theta_i(t)\right)\mathrm{d}t, \tag{7b}$$

$$\mathrm{d}\theta_i(t) = \omega_i(t)\mathrm{d}t, \tag{7c}$$

$$\mathrm{d}v_i(t) = \frac{1}{m_i}F_i(t)\mathrm{d}t + \sigma_i^F\left(v_i(t)\right)\mathrm{d}W_i^F(t), \tag{7d}$$

$$\mathrm{d}\omega_i(t) = \frac{1}{I_i}\tau_i(t)\mathrm{d}t + \sigma_i^\tau\left(\omega_i(t)\right)\mathrm{d}W_i^\tau(t), \tag{7e}$$

for $i = 1, \dots, N$, where $p_i = [x_i, y_i]^T$ is the inertial position of the i-th robot, θ_i its steering angle, v_i its linear speed, ω_i its turn rate, m_i its mass, $I_i(t)$ its moment of inertia, τ_i the applied torque, F_i the applied force; W_i^F and W_i^τ are two mutually independent Wiener processes representing the noise acting on the i-th robot speed and angular velocity with intensities σ_i^F and σ_i^τ respectively. Notice that the increments $\mathrm{d}W_i^F(t)$ and $\mathrm{d}W_i^\tau(t)$ are normally distributed random variables with variance $\mathrm{d}t$.

In Eq. (7d), the stochastic term $\sigma_i^F(v_i)\mathrm{d}W_i^F(t)$ captures possible uncertainties in the actuation of the input force to robot i, which may be induced by fluctuations of the actuators' power supply, or by unmodeled friction forces. The term $\sigma_i^\tau(\omega_i)\mathrm{d}W_i^\tau(t)$ in Eq. (7e) captures uncertainties in the actuation of the input torque of the i-th robot, which may be related to external disturbances such as wind gusts, robot chassis shaking, or vibration due to off-road rough surface or other environmental factors. In what follows, we consider that the noise intensities $\sigma_i^F(v_i)$ and $\sigma_i^\tau(\omega_i)$ fulfill the following assumption:

Assumption III.1. *The noise intensity functions σ_i^F and σ_i^τ are globally Lipschitz with respect to v_i and ω_i, respectively, that is, there exists a positive scalar κ such that*

$$\begin{aligned}\left\|\sigma_i^F(\alpha) - \sigma_i^F(\beta)\right\|_2 &\leq \kappa\left\|\alpha - \beta\right\|_2, \\ \left\|\sigma_i^\tau(\alpha) - \sigma_i^\tau(\beta)\right\|_2 &\leq \kappa\left\|\alpha - \beta\right\|_2,\end{aligned} \tag{8}$$

for all $\alpha, \beta \in \mathbb{R}$, $i = 1, \dots, N$. Furthermore, they are zero at the origin, and there exist two positive scalars $\sigma_{\max}^F$ and $\sigma_{\max}^\tau$ such that $|\sigma_i^F| \leq \sigma_{\max}^F$ and $|\sigma_i^\tau| \leq \sigma_{\max}^\tau$, respectively.

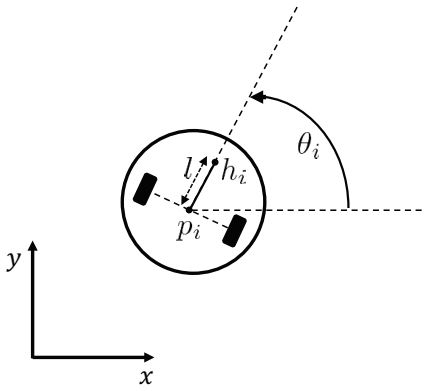

Fig. 1. Differential wheeled robot i with inertial position p_i, steering angle θ_i, and hand position h_i at a distance l from the inertial position.

Assuming a bound on the noise intensity is a tenable assumption and is consistent with the experimental evidence, see the Supplementary Information. Different value of this bound may impact on the stability properties of the system under analysis. For instance, in harmonic oscillators with fluctuating damping [62], [63], variations of the noise intensity may generate a negative effective dumping, thus yielding instability. In our study on groups of mobile robots, we will evaluate how a variation of $\sigma_{\max}^F$ and $\sigma_{\max}^\tau$ affects system performance, and thus the achievement of the desired formation.

B. Formation control goal

In this work, rather than focusing on coordinating the inertial position of the robots, we control their hand position, that is, the position of a point $h = [h_x, h_y]^T$ at a distance l from the inertial position along the line normal to the wheel axes that intersects it at its center, see Figure 1. Indeed, the coordination of the hand position is often of interest from a practical standpoint, think for instance of robots equipped with a gripper to jointly move large objects, or the coordinated placement of sensors mounted at the hand position of each robot [37], [64]–[67]. Formally, denoting h_i the hand position of the i-th robot, we can write

$$h_i(t) = \begin{bmatrix} h_{xi}(t) \\ h_{yi}(t) \end{bmatrix} = \begin{bmatrix} x_i(t) \\ y_i(t) \end{bmatrix} + l\begin{bmatrix} \cos\left(\theta_i(t)\right) \\ \sin\left(\theta_i(t)\right) \end{bmatrix}. \tag{9}$$

Here, we consider the problem of controlling the robots so that a sequence of locations $\mathcal{H}_\ell$, $\ell = 1, \dots, m$, are visited by the robots' hands. Specifically, the ℓ-th location is defined as

$$\mathcal{H}_\ell = \left\{\bar{h}_1^\ell, \dots, \bar{h}_N^\ell\right\},$$

where $\bar{h}_i^\ell$ is the desired position of the hand of the i-th robot at the ℓ-th location.

We assume that the set of nodes $\mathcal{V}$ can be partitioned in the subset of the *followers* $\mathcal{V}_F$ and that of the *leaders* $\mathcal{V}_L$. The followers are only aware of the desired relative hand position with respect to neighboring agents. Additionally, each leader $i \in \mathcal{V}_L$ is also aware of the sequence of desired positions for its own hand, that is, of $\bar{h}_i^1, \ldots, \bar{h}_i^m$, and can measure the relative hand position with respect to its current desired location, say the ℓ-th, defined as $\zeta_i = h_i - \bar{h}_i^\ell$. The control goal is twofold: i) moving the robots towards the specified sequence of locations $\mathcal{H}_1, \ldots, \mathcal{H}_m$ and ii) achieving and maintaining the desired formation, that is, at a given location ℓ of the formation pattern, guaranteeing that $h_i - h_j$ converges towards $\bar{h}_i^\ell - \bar{h}_j^\ell$ for all $i, j = 1, \ldots, N$. We can then define the *formation stabilization error* as

$$e(t) = e_l(t) + e_f(t), \tag{10}$$

where $e_l := \sum_{i=1}^N \zeta_i^T C_p \zeta_i$ is the *location error*, defined as the square of the weighted norm of the mismatch between the current hand position of the robots and the current desired location, with $C_p = C_p^T > 0$ being the weighting matrix, while

$$e_f := \sum_{(i,j)\in\mathcal{E}} (\zeta_i - \zeta_j)^T K_p (\zeta_i - \zeta_j)$$

is the *formation error*, with weighting matrix $K_p = K_p^T > 0$. C_p and K_p are selected to balance the relevance of maintaining the formation against the requirement of achieving the desired location. Notice that $e(t) = 0$ if and only if $\zeta_i(t) = 0$ for all $i = 1, \ldots, N$.

Definition III.2. *We say that system* (15) *converges almost surely (a.s.) to the desired formation if the formation stabilization error converges a.s. to zero, that is,*

$$\lim_{t\to+\infty} e(t) = 0 \quad \textit{almost surely.}$$

Remark III.3. *The proposed leader-follower control scheme is cost-efficient, as only leaders need to use navigation sensors such as LIDAR for Simulatneous Localization and Mapping (SLAM) or Global Positioning System (GPS), to follow the path [68]. Followers can only rely on cheap proximity sensors to achieve the formation pattern. This might result in unpredictable and uncertain perturbations in the control actuation force and torque, thus necessitating the use of stochastic SDEs to model it.*

C. Reduction of the input-output dynamics

As our final goal is to regulate the hands' dynamics, we can view (9) as the output equation of system (7), and, extending the procedure implemented in [37], we can design the control inputs so as to output feedback linearize the deterministic part of the system dynamics. For compactness of notation, in all the derivations that follows we shall omit explicit dependence on time when apparent. Now, we notice that, by applying the Itô's formula (5) to (9), and observing that no-noise is directly acting on x_i, y_i, and θ_i,

$$\mathrm{d}h_i = z_i \mathrm{d}t, \tag{11}$$

where

$$z_i = \begin{bmatrix} z_{i1} \\ z_{i2} \end{bmatrix} = \begin{bmatrix} v_i \cos(\theta_i) - l\omega_i \sin(\theta_i) \\ v_i \sin(\theta_i) + l\omega_i \cos(\theta_i) \end{bmatrix}.$$

Next, by applying the Itô's formula to z_i, and denoting $\varrho = [v_i, \omega_i, \theta_i]^T$ we obtain

$$\begin{aligned} \mathrm{d}z_{i1} = \Bigg(& \frac{\partial z_{i1}}{\partial t} + \frac{\partial z_{i1}}{\partial \varrho} f(\varrho) \\ & + \mathrm{trace}\left(g^T(\varrho) \frac{\partial^2 z_{i1}}{\partial \varrho^2} g(\varrho) \right) \Bigg) \mathrm{d}t + \frac{\partial z_{i1}}{\partial \varrho} g(\varrho) \mathrm{d}W_i \end{aligned} \tag{12}$$

where

$$g(\varrho) = \begin{bmatrix} \sigma_i^F & 0 \\ 0 & \sigma_i^\tau \\ 0 & 0 \end{bmatrix}, f(\varrho) = \begin{bmatrix} F_i/m_i \\ \tau_i/I_i \\ \omega_i \end{bmatrix}, W_i = \begin{bmatrix} W_i^F \\ W_i^\tau \end{bmatrix}. \tag{13}$$

Now, computing $\partial^2 z_{i1}/\partial \varrho^2$, we obtain

$$\begin{bmatrix} 0 & 0 & -\sin(\theta_i) \\ 0 & 0 & -l\cos(\theta_i) \\ -\sin(\theta_i) & -l\cos(\theta_i) & -v_i\cos(\theta_i) + l\omega_i \sin(\theta_i) \end{bmatrix},$$

which, together with (13), yields

$$\mathrm{trace}\left(g^T(\varrho) \frac{\partial^2 z_{i1}}{\partial \varrho^2} g(\varrho) \right) = 0.$$

Noting that $\partial z_{i1}/\partial t = 0$, and $\partial z_{i1}/\partial \varrho = [\cos(\theta_i), -l\sin(\theta_i), -v_i \sin(\theta_i) - l\omega_i \cos(\theta_i)]^T$, we have that (12) becomes

$$\begin{aligned} \mathrm{d}z_{i1} = & \left(-v_i\omega_i \sin(\theta_i) - l\omega_i^2 \cos(\theta_i) \right) \mathrm{d}t \\ & + \left(\frac{\cos(\theta_i)}{m_i} F_i - \frac{l\sin(\theta_i)}{I_i} \tau_i \right) \mathrm{d}t \\ & + \left[\sigma_i^F \cos(\theta_i), -l\sigma_i^\tau \sin(\theta_i) \right] \begin{bmatrix} \mathrm{d}W_i^F \\ \mathrm{d}W_i^\tau \end{bmatrix}. \end{aligned}$$

Following similar steps for the computation of $\mathrm{d}z_{i2}$, we finally get

$$\begin{aligned} \mathrm{d}z_i = & \begin{bmatrix} -v_i\omega_i \sin(\theta_i) - l\omega_i^2 \cos(\theta_i) \\ v_i\omega_i \cos(\theta_i) - l\omega_i^2 \sin(\theta_i) \end{bmatrix} \mathrm{d}t \\ & + \begin{bmatrix} \frac{1}{m_i}\cos(\theta_i) & -\frac{l}{I_i}\sin(\theta_i) \\ \frac{1}{m_i}\sin(\theta_i) & \frac{l}{I_i}\cos(\theta_i) \end{bmatrix} u_i(t) \mathrm{d}t \\ & + \begin{bmatrix} \sigma_i^F(v_i)\cos(\theta_i) & -l\sigma_i^\tau(\omega_i)\sin(\theta_i) \\ \sigma_i^F(v_i)\sin(\theta_i) & l\sigma_i^\tau(\omega_i)\cos(\theta_i) \end{bmatrix} \begin{bmatrix} \mathrm{d}W_i^F \\ \mathrm{d}W_i^\tau \end{bmatrix}, \end{aligned}$$

Then, we can introduce and apply the following diffeomorphism $\psi : \mathbb{R}^5 \to \mathbb{R}^5$ [69]:

$$\chi_i = \psi(s_i) = \begin{bmatrix} x_i + l\cos(\theta_i) \\ y_i + l\sin(\theta_i) \\ v_i\cos(\theta_i) - l\omega_i\sin(\theta_i) \\ v_i\sin(\theta_i) + l\omega_i\cos(\theta_i) \\ \theta_i \end{bmatrix}, \tag{14}$$

where $s_i = \begin{bmatrix} x_i, y_i, \theta_i, v_i, \omega_i \end{bmatrix}^T$ is the full state of robot i in the inertial frame. We thus obtain the state vector χ_i of robot i associated to the robot's hand, which is what we aim at controlling. The dynamics of hand of the i-th robot can be then written as

$$\mathrm{d}\chi_{i1} = \chi_{i3}\mathrm{d}t, \tag{15a}$$

$$\mathrm{d}\chi_{i2} = \chi_{i4}\mathrm{d}t, \tag{15b}$$

$$\begin{aligned} \begin{bmatrix} \mathrm{d}\chi_{i3} \\ \mathrm{d}\chi_{i4} \end{bmatrix} &= \begin{bmatrix} -v_i\omega_i\sin(\theta_i) - l\omega_i^2\cos(\theta_i) \\ v_i\omega_i\cos(\theta_i) - l\omega_i^2\sin(\theta_i) \end{bmatrix}\mathrm{d}t \\ &+ \begin{bmatrix} \frac{1}{m_i}\cos(\theta_i(t)) & -\frac{l}{I_i}\sin(\theta_i(t)) \\ \frac{1}{m_i}\sin(\theta_i) & \frac{l}{I_i}\cos(\theta_i) \end{bmatrix} u_i\mathrm{d}t \\ &+ \begin{bmatrix} \sigma_i^F(v_i)\cos(\theta_i) & -l\sigma_i^\tau(\omega_i)\sin(\theta_i) \\ \sigma_i^F(v_i)\sin(\theta_i) & l\sigma_i^\tau(\omega_i)\cos(\theta_i) \end{bmatrix} \begin{bmatrix} \mathrm{d}W_i^F \\ \mathrm{d}W_i^\tau \end{bmatrix}, \end{aligned} \tag{15c}$$

$$\mathrm{d}\chi_{i5} = \left(-\frac{1}{l}\chi_{i3}\sin(\chi_{i5}) + \frac{1}{l}\chi_{i4}\cos(\chi_{i5}) \right)\mathrm{d}t, \tag{15d}$$

where $u_i(t) = [F_i(t), \tau_i(t)]^T$, for all $i = 1, \ldots, N$. [1] Observing that

$$\det \begin{bmatrix} \frac{1}{m_i}\cos(\theta_i) & -\frac{l}{I_i}\sin(\theta_i) \\ \frac{1}{m_i}\sin(\theta_i) & \frac{l}{I_i}\cos(\theta_i) \end{bmatrix} = \frac{l}{m_i I_i} \neq 0,$$

we can then choose

$$\begin{aligned} u_i = \begin{bmatrix} \frac{1}{m_i}\cos(\theta_i) & -\frac{l}{I_i}\sin(\theta_i) \\ \frac{1}{m_i}\sin(\theta_i) & \frac{l}{I_i}\cos(\theta_i) \end{bmatrix}^{-1} \Bigg[\varphi_i \\ - \begin{pmatrix} -v_i\omega_i\sin(\theta_i) - l{\omega_i}^2\cos(\theta_i) \\ v_i\omega_i\cos(\theta_i) - l{\omega_i}^2\sin(\theta_i) \end{pmatrix} \Bigg], \end{aligned} \tag{16}$$

which, together with (15c), yields

$$\begin{aligned} \begin{bmatrix} \mathrm{d}\chi_{i3} \\ \mathrm{d}\chi_{i4} \end{bmatrix} &= \varphi_i\mathrm{d}t \\ &+ \begin{bmatrix} \sigma_i^F(v_i)\cos(\chi_{i5}) & -l\sigma_i^\tau(\omega_i)\sin(\chi_{i5}) \\ \sigma_i^F(v_i)\sin(\chi_{i5}) & l\sigma_i^\tau(\omega_i)\cos(\chi_{i5}) \end{bmatrix} \begin{bmatrix} \mathrm{d}W_i^F \\ \mathrm{d}W_i^\tau \end{bmatrix}, \end{aligned} \tag{17}$$

where φ_i is a decentralized control input to be selected. Hence, the linear operator in (14) allows to reduce the input-output dynamics of individual robot to the stochastic double integrator in (15a), (15b), and (17). Thus, to control the hand position of the differential drive robot i, it suffices to design an appropriate control law φ_i. Finally, note that, by computing the inverse in (16), one obtains that the control gains are proportional to m_i/l and I_i/l, respectively. Therefore, if the hand were too close to the inertial position, thus making l small compared to the mass and moment of inertia of the robot, a careful design of φ_i would be needed to prevent potentially high values of the control gains.

[1] Equation (15d) has been obtained by noticing that $\mathrm{d}\chi_{i5} = \omega_i\mathrm{d}t$, and then expressing ω_i as a function of χ_{i3}, χ_{i4} and χ_{i5} by means of equation (14).

IV. Control Design

Notice that, by introducing the vector $\eta_i = \begin{bmatrix} \chi_{i3}, \chi_{i4} \end{bmatrix}^T$, and from equation (15), the dynamics of the relative hand position error ζ_i can be written as

$$\mathrm{d}\begin{bmatrix} \zeta_i(t) \\ \eta_i(t) \end{bmatrix} = \begin{bmatrix} \eta_i(t) \\ \varphi_i(t) \end{bmatrix}\mathrm{d}t + \begin{bmatrix} 0_{2\times 2} \\ \Omega_i(t) \end{bmatrix}\mathrm{d}W_i(t), \tag{18}$$

for $i = 1, \ldots, N$, where $W_i = \begin{bmatrix} W_i^F(t), W_i^\tau(t) \end{bmatrix}^T$ and

$$\Omega_i(t) = \begin{bmatrix} \sigma_i^F(v_i)\cos(\chi_{i5}(t)) & -l\sigma_i^\tau(\omega_i)\sin(\chi_{i5}(t)) \\ \sigma_i^F(v_i)\sin(\chi_{i5}(t)) & l\sigma_i^\tau(\omega_i)\cos(\chi_{i5}(t)) \end{bmatrix}. \tag{19}$$

In compact matrix form, we can rewrite (18) as

$$\mathrm{d}\begin{bmatrix} \zeta(t) \\ \eta(t) \end{bmatrix} = f\left(\zeta(t), \eta(t)\right)\mathrm{d}t + g(t)\mathrm{d}W, \tag{20}$$

where $\zeta = \begin{bmatrix} \zeta_1^T, \ldots, \zeta_N^T \end{bmatrix}^T$, $\eta = \begin{bmatrix} \eta_1^T, \ldots, \eta_N^T \end{bmatrix}^T$, $f\left(\zeta(t), \eta(t)\right) = [\eta(t)^T, \varphi\left(\zeta(t), \eta(t)\right)^T]^T$, $W = [W_1^T, \ldots, W_N^T]^T$, and $g(t) = \begin{bmatrix} 0_{2N\times 2N}, \Omega(t)^T \end{bmatrix}^T$, with $\Omega = \mathrm{diag}\left(\Omega_1, \ldots, \Omega_N\right)$ and $\varphi = \begin{bmatrix} \varphi_1^T, \ldots, \varphi_N^T \end{bmatrix}^T$. Here, we propose a decentralized control action to achieve the desired formation. Namely, the control input to the followers is

$$\varphi_i = -\sum_{j=1}^{N} a_{ij}w_{ij}\left(K_p\left(\zeta_i - \zeta_j\right) + K_v\left(\eta_i - \eta_j\right)\right), \tag{21}$$

for all $i \in \mathcal{V}_F$, where K_p and K_v are symmetric positive definite matrices defining the control gains for the group cohesion and alignment terms, respectively. The control input to the leaders will have an additional term to leverage the information on the desired location. Namely,

$$\begin{aligned} \varphi_i = &- C_p\zeta_i - C_v\eta_i \\ &- \sum_{j=1}^{N} a_{ij}w_{ij}\left(K_p\left(\zeta_i - \zeta_j\right) + K_v\left(\eta_i - \eta_j\right)\right), \end{aligned} \tag{22}$$

for all $i \in \mathcal{V}_L$, where C_p and C_v are symmetric positive definite matrices gains weighting the terms inducing the

desired formation pattern.[2] Note that C_p and K_p are chosen to be identical to the weighting matrix defined in the formation stabilization error in equation (10). In compact matrix form, the control law (21)-(22) can be rewritten as

$$\varphi = \varphi\left(\zeta(t), \eta(t)\right) = -M_1\zeta(t) - M_2\eta(t). \tag{23}$$

where $M_1 = U \otimes C_p + L \otimes K_p$ and $M_2 = U \otimes C_v + L \otimes K_v$, with U being a diagonal matrix whose i-th element is 1 if $i \in \mathcal{V}_L$, while it is 0 otherwise. Note that, as the graph $\mathcal{G}$ is undirected and connected, M_1 and M_2 are symmetric and positive definite by construction [70]. Before giving our main result, we prove the following useful Lemma:

Lemma IV.1. *If* $\lim_{t+\infty} \eta(t) = 0$ *a.s., then*

1) $\lim_{t+\infty} \mathrm{d}\zeta(t) = 0$ *a.s.;*
2) $\lim_{t+\infty} \zeta(t) = 0$ *a.s.;*
3) $\lim_{t+\infty} \mathrm{d}\eta(t) = 0$ *a.s.*

Proof. From (18),

$$\mathrm{d}\zeta(t) = \eta(t)\mathrm{d}t.$$

Then, taking the limit for $t \to +\infty$, point 1) trivially follows. In turn, this implies

$$\lim_{t+\to\infty} \zeta(t) = \bar{\zeta} \text{ a.s.}, \tag{24}$$

for some constant vector $\bar{\zeta} \in \mathbb{R}^{2N}$.

Next, we show that $\bar{\zeta} = 0$ by contradiction. Indeed, let us assume that $\bar{\zeta} \neq 0$. From equation (20), and taking the limit for $t \to +\infty$, as $\lim_{t\to+\infty} \eta(t) = 0$ we obtain

$$\lim_{t\to+\infty} \mathrm{d}\eta(t) = \lim_{t\to+\infty} -M_1\bar{\zeta}\mathrm{d}t + \Omega(t)\mathrm{d}W \text{ a.s.} \tag{25}$$

Notice that

$$\eta_i(t) = \begin{bmatrix} v_i(t)\cos\left(\theta_i(t)\right) - l\omega_i(t)\sin\left(\theta_i(t)\right) \\ v_i(t)\sin\left(\theta_i(t)\right) + l\omega_i(t)\cos\left(\theta_i(t)\right) \end{bmatrix}, \tag{26}$$

for all $i = 1, \ldots, N$. As $\lim_{t\to+\infty} \eta(t) = 0$ a.s., this implies that

$$\lim_{t\to+\infty} v_i(t) = 0 \text{ a.s., and } \lim_{t\to+\infty} \omega_i(t) = 0 \text{ a.s.} \tag{27}$$

From the definition (19) of Ω_i, this implies that

$$\lim_{t\to+\infty} \Omega(t) = 0. \text{ a.s.} \tag{28}$$

By combining (28) with (25), we obtain

$$\lim_{t\to+\infty} \mathrm{d}\eta(t) = -M_1\bar{\zeta}\mathrm{d}t \text{ a.s.} \tag{29}$$

[2]Since collisions might occur when the formation is tight, the controller can be completed by an additive collision avoidance term ∇J_i obtained by evaluating the gradient of a potential function J_i which can be defined e.g. as in [47].

As we assumed $\bar{\zeta} \neq 0$, since M_1 is non-singular, we must also have $-M_1\bar{\zeta} \neq 0$, and therefore $\mathrm{d}\eta(t)$ in the limit would be equal to a non-zero constant vector, thus contradicting the hypothesis that $\lim_{t\to+\infty} \eta(t) = 0$. This contradicts the assumption, and therefore $\bar{\zeta} = 0$, thus proving points 2) and 3). □

We are now ready to give the following result:

Theorem IV.2. *Under the control law* (16)*,* (23)*, if Assumption III.1 holds and* $\lambda_1(M_2) > \kappa^2/2$*, then system* (15) *converges almost surely to the desired formation.*

Proof. We start by showing that all the three assumptions of Lemma II.2 for the error system (20) hold. Indeed,

1) f is linear and continuously differentiable. Furthermore, as Assumption III.1 holds, then Assumption II.1 is fulfilled, too.
2) Assumption III.1 also implies that g is bounded.
3) Let us introduce the following function $V \in C^{2,1}\left(\mathbb{R}^{4N} \times \mathbb{R}^+, \mathbb{R}^+\right)$:

$$V(\zeta, \eta) = \frac{1}{2}\zeta^T\left(U \otimes C_p + L \otimes K_p\right)\zeta + \frac{1}{2}\eta^T\eta. \tag{30}$$

By defining $\gamma := [\zeta(t)^T \ \eta(t)^T]^T$, and since $M_1 > 0$, we have

$$\lim_{\|\gamma\|_2\to+\infty} \inf_{t\in\mathbb{R}^+} V(\gamma) = \lim_{\|\gamma\|_2\to+\infty} V(\gamma) = +\infty, \tag{31}$$

and thus (4a) is fulfilled. Next, we can write

$$\begin{aligned} \mathcal{L}V(\gamma) &= \frac{\partial V}{\partial \gamma} f(\gamma) + \frac{1}{2}\mathrm{trace}\left(g^T \frac{\partial^2 V}{\partial \gamma^2} g\right) \\ &= \frac{\partial V}{\partial \gamma}\begin{bmatrix} \eta \\ \varphi(\zeta, \eta) \end{bmatrix} \\ &+ \frac{1}{2}\mathrm{trace}\left(\begin{bmatrix} 0_{2N\times 2N} & \Omega^T \end{bmatrix} \frac{\partial^2 V}{\partial \gamma^2}\begin{bmatrix} 0_{2N\times 2N} \\ \Omega \end{bmatrix}\right). \end{aligned} \tag{32}$$

Now, considering that

$$\frac{\partial V}{\partial \gamma} = \begin{bmatrix} \zeta^T\left(U \otimes C_p + L \otimes K_p\right) & \eta^T \end{bmatrix} \tag{33a}$$

and

$$\frac{\partial^2 V}{\partial \gamma^2} = \begin{bmatrix} U \otimes C_p + L \otimes K_p & O_{2N\times 2N} \\ O_{2N\times 2N} & I_{2N\times 2N} \end{bmatrix}, \tag{33b}$$

by exploiting the symmetry of C_p and K_p, we finally get

$$\begin{aligned} \mathcal{L}V = &-\eta^T\left(U \otimes C_v + L \otimes K_v\right)\eta \\ &+ \frac{1}{2}\sum_{i=1}^{N}\left(\left(\sigma_i^F(v_i)\right)^2 + \left(l\sigma_i^\tau(\omega_i)\right)^2\right). \end{aligned} \tag{34}$$

From Assumption III.1, we know that

$$\sum_{i=1}^{N}\left(\left(\sigma_i^F(v_i)\right)^2+\left(l\sigma_i^\tau(\omega_i)\right)^2\right) \leq \sum_{i=1}^{N}\left(\kappa^2\left(v_i^2+l^2\omega_i^2\right)\right). \tag{35}$$

Furthermore, computing the inverse of the operator ψ defined in (14) yields

$$\begin{aligned} v_i &= \chi_{i3}\cos(\chi_{i5})+\chi_{i3}\sin(\chi_{i5}),\\ \omega_i &= -\frac{1}{l}\chi_{i3}\sin(\chi_{i5})+\frac{1}{l}\chi_{i4}\cos(\chi_{i5}). \end{aligned} \tag{36}$$

Combining (35) and (36), we obtain

$$\begin{aligned} &\sum_{i=1}^{N}\left(\left(\sigma_i^F(v_i)\right)^2+\left(l\sigma_i^\tau(\omega_i)\right)^2\right)\\ &\leq \sum_{i=1}^{N}\left(\kappa^2\left(\chi_{3i}^2+\chi_{4i}^2\right)\right)=\kappa^2\eta^T\eta, \end{aligned} \tag{37}$$

thus yielding

$$\begin{aligned} \mathcal{L}V &\leq -\eta^T\left(U\otimes C_p+L\otimes K_p\right)\eta+\frac{\kappa^2}{2}\eta^T\eta,\\ &\leq -\lambda_1(M_2)\eta^T\eta+\frac{\kappa^2}{2}\eta^T\eta\\ &= \left(\frac{\kappa^2}{2}-\lambda_1(M_2)\right)\eta^T\eta := \mu(\eta). \end{aligned} \tag{38}$$

As from the hypothesis of the Theorem we have $\lambda_1(M_2) > \kappa^2/2$, and from Assumption III.1, the third and last hypothesis of Lemma II.2 also holds. Now, from the thesis of Lemma II.2, we have

$$\lim_{t\to+\infty} V(\gamma) \text{ exists and is finite almost surely.} \tag{39}$$

Furthermore, $\lim_{t\to+\infty}\mu(\eta)=0$ a.s., which implies that

$$\lim_{t\to+\infty}\eta(t)=0 \text{ almost surely.} \tag{40}$$

From Lemma IV.1, the thesis follows. □

Remark IV.3. *Notice that to check the sufficient condition provided in Theorem IV.2, it is necessary to compute the smallest eigenvalue of matrix M_2. Although the latter is related to the overall network structure, encoded by the graph Laplacian, a distributed algorithm that only leverages local information can be employed to estimate $\lambda_1(M_2)$ [71].*

Remark IV.4. *Note that, in the absence of noise, if the network topology is an unweighted ring (that is, by setting $w_{ij}=1$, $a_{i-1,i}=a_{i,i+1}=1$ and $a_{ij}=0$), and all the nodes have full knowledge of the target location ($\mathcal{V}=\mathcal{V}_L$), then our control law* (16), (23) *coincides with that introduced in [37], and the convergence towards the desired location is not anymore in a probabilistic sense, but becomes asymptotic.*

Interestingly, the sufficient condition for the almost sure convergence of the robot formation towards the desired trajectory depends on the noise intensity functions through the parameter κ, the network topology through matrix M_2, and the matrix control gains C_v and K_v. The following corollary further highlights these relationships.

Corollary IV.4.1. *If $C_v = bK_v$ for some positive scalar b and $\lambda_1(bU+L)\lambda_1(K_v) > \kappa^2/2$, then system* (15) *converges almost surely to the desired formation.*

Proof. Notice that, when $C_v = bK_v$, we can write $M_2 = (bU+L)\otimes C_v$. Then, from the properties of the Kronecker product,

$$\lambda_1(M_2)=\lambda_1(bU+L)\lambda_1(K_v). \tag{41}$$

From Theorem IV.2, the thesis follows. □

Remark IV.5. *In our theoretical derivation, we consider the scenario in which the network topology of the controlled networked system is undirected, that is, if agent i is a neighbor of agent j, then j is also a neighbor of i, thus implying a symmetric Laplacian matrix. We emphasize that, in the presence of different schemes yielding to a directed Laplacian matrix [72], which may arise, for instance, when the agents are equipped with proximity sensors with different ranges, our approach could be extended by leveraging the theory on M-matrices, see e.g. [73].*

V. Numerical Analysis

In this section, we conduct a numerical study to validate the theoretical findings of Section IV and to offer further insights on the relevance of the network topology, the control parameters, and the noise intensity on the fulfillment of the formation task.

A. Discrete-time approximation

To perform the numerical analysis and allow for the subsequent implementation on ground robots, we used a discrete-time approximation [74], [75] of the stochastic

robot hand dynamics (15), (18) using the standard Euler-Maruyama method [76], which yields

$$\begin{aligned}\zeta_i(k+\Delta t) &= \zeta_i(k) + \eta_i(k)\Delta t\\ \eta_i(k+\Delta t) &= \eta_i(k) + \varphi_i(k)\Delta t + \Omega_i(k)\Delta W_i(k),\\ \chi_{i5}(k+\Delta t) &= \chi_{i5}(k) + \bigg(-\frac{1}{2l}\eta_{i1}(k)\sin\left(\chi_{i5}(k)\right)\\ &\quad + \frac{1}{2l}\eta_{i2}(k)\cos\left(\chi_{i5}(k)\right)\bigg)\Delta t,\end{aligned} \tag{42}$$

for $i = 1, \ldots, N$, where Δt is the discrete time increment, and $\Delta W_i(k) = \left[\Delta W_i^F(k), \Delta W_i^\tau(k)\right]^T$, with $\Delta W_i^F(k) = W_i^F(k+1) - W_i^F(k)$ and $\Delta W_i^\tau(k) = W_i^\tau(k+1) - W_i^\tau(k)$, respectively. Notice that the random variables $\Delta W_i^F(k)$ and $\Delta W_i^\tau(k)$ are independent normally distributed with zero mean and variance Δt.

To simulate the time behavior of the inertial position of the robots, from equation (14) we can compute the linear speed v_i and turn rate ω_i as

$$\begin{bmatrix} v_i(k) \\ \omega_i(k) \end{bmatrix} = \begin{bmatrix} \cos\left(\chi_{i5}(k)\right) & -l\sin\left(\chi_{i5}(k)\right) \\ \sin\left(\chi_{i5}(k)\right) & l\cos\left(\chi_{i5}(k)\right) \end{bmatrix}^{-1} \eta_i(k), \tag{43}$$

thus obtaining

$$\begin{aligned} x_i(k+\Delta t) &= x_i(k) + v_i(k)\cos(\chi_{i5}(k))\Delta t,\\ y_i(k+\Delta t) &= y_i(k) + v_i(k)\sin(\chi_{i5}(k))\Delta t. \end{aligned} \tag{44}$$

B. Numerical setup

In our numerical analyses, the control objective is to steer a formation of $N = 10$ planar robots towards a desired configuration $\mathcal{H}_1 = \left\{\mathcal{H}_1^1, \ldots, \mathcal{H}_1^N\right\}$, where $\mathcal{H}_1^i$ is the desired hand position of the i-th robot. In particular, we focus on the problem of achieving a balanced circular formation, which is a traditional testbed problem in the literature on multi-agent systems [77], and therefore we select the positions $\mathcal{H}_1^i$, $i = 1, \ldots, 10$, accordingly. Specifically, the agents have to be balanced on a circle of center $(5, 5)$ and radius 1.5, hence the desired position of robot 1 is randomly set on the circle, while those of the remaining robots are successively set on the circle at π/N degrees from the previous one. The robots are coupled through a ring network, and thus the off-diagonal elements of the associated Laplacian matrix are defined as $l_{ij} = -1$ if $|j - i| \in \{1, N-1\}$, while they are 0 otherwise. As a worst case scenario, we consider the case in which only one node is a leader. [3] Specifically, node 1 is elected to be the only network leader, and therefore the only non-zero diagonal element of the matrix U, introduced after equation (23), is the first one. Furthermore, the individual robot parameters are taken consistently with the specifications of the customized ground robots we used for the subsequent experimental validation (*iRobot Create 2, iRobot Corporation, Bedford, MA, USA*). Namely, we selected $l = 0.15\,\mathrm{m}$, $m_i = 4.99\,\mathrm{Kg}$, and $I_i = 0.13\,\mathrm{Kg\,m^2}$, for all $i = 1, \ldots, N$. The matrix control gains are selected as multiples of the identity matrix, that is,

$$C_v = c_v I_2, \quad K_v = k_v I_2, \quad C_p = c_p I_2, \quad K_p = k_p I_2, \tag{45}$$

where c_v, k_v, c_p, and k_p are positive scalar control gains, whereas the noise intensity functions, in agreement with the model validation performed in the Supplementary Information, are selected as

$$\sigma_i^F(v_i) = s_F \tanh(v_i), \qquad \sigma_i^\tau(\omega_i) = s_\tau \tanh(\omega_i), \tag{46}$$

for all $i = 1, \ldots, N$, with s_F and s_τ being positive scalars. At the onset of each simulation, the position of each robot is drawn randomly in a circular domain of radius 2 centered at the origin, while its initial heading is randomly drawn in the interval $[-\pi, \pi]$. We set the discrete time step Δt in (42)-(44) to 0.01s, and the total simulation time to $T = 500\,\mathrm{s}$.

C. Results

In our investigation, we first perform two representative simulations to illustrate the effectiveness of the sufficient condition in Theorem IV.2, where we set all the scalar gains in (45) to 1, thus yielding $\lambda_1(M_2) = 1$. In the first simulation, the sufficient condition for convergence is fulfilled, as we select $s_F = 1$ and $s_\tau = 1$ in (46), and therefore $\kappa^2/2 = 0.5 < \lambda_1(M_2)$. According to the theoretical prediction, in Figure 2(a) we observe convergence towards the formation objective. Figure 2(b) then reports the results of a second representative simulation in which the sufficient conditions in Theorem IV.2 are not satisfied ($s_F = s_\tau = 5 = \kappa > \lambda_1(M_2)$) and convergence is not achieved.

Next, we study the influence of the design parameters on the convergence and stability of the multi-agent system by varying the scalar control gains c_v, k_v, and c_p, k_p in equation (45), and the maximum noise intensities s_F and s_τ in (46). To this aim, we set $N = 4$ and define the convergence time t_c as

$$t_c = \min \mathcal{T} := \{t \in \mathbb{R}^+ : |e(\tau)| < 10^{-6}\, \forall \tau > t\}.$$

When $\mathcal{T} = \emptyset$, we set $t_c = +\infty$. In Figure 3, three colormaps describe the variation of t_c when the control

[3] Indeed, if more leaders are added in the network $\lambda_1(M_2)$ may only increase, see e.g. [70]. From Theorem IV.2, this means that larger values of κ can be considered, and therefore the control action is capable of compensating for larger classes of noise intensity functions, see Assumption III.1.

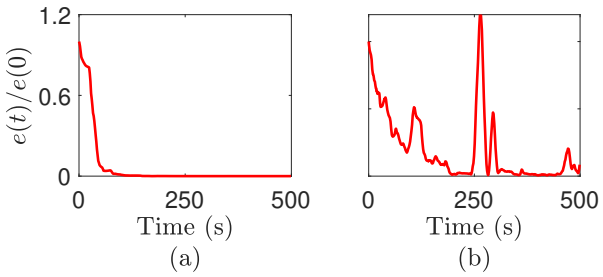

Fig. 2. Time evolution of the normalized formation error $e(t)/e(0)$ when (a) $s_F = 1, s_\tau = 1$ and (b) $s_F = 5, s_\tau = 5$, respectively.

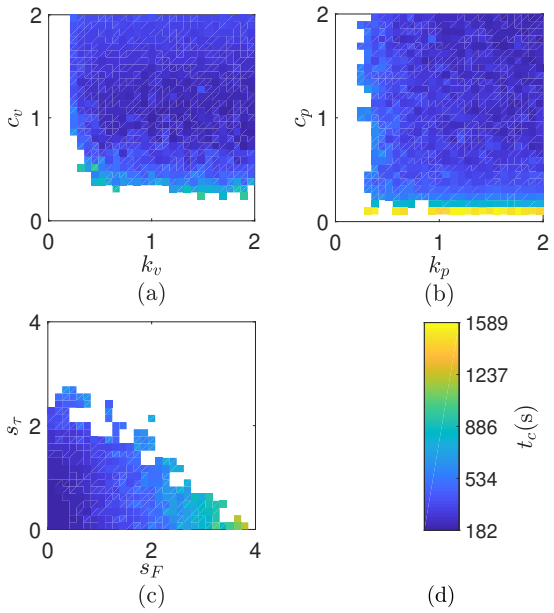

Fig. 3. Averaged convergence time t_c as a function of (a) the gains c_v and k_v in (45), (b) c_p and k_p in (45), (c) the noise intensities s_F and s_τ in (46). Each pixel is obtained by averaging t_c over 30 simulated trajectories. White pixels correspond to $t_c \to +\infty$ in at least one of the 30 repetitions. The color scale used for displaying the convergence time (t_c) is illustrated in panel (d).

gains and the noise intensities are varied. Each dot in the colormaps is the outcome of an average over 30 simulations. White areas in the map correspond to $t_c = +\infty$. In Figures 3(a) and 3(b) we illustrate the dependency of the convergence time on the control gains. Specifically, in Figure 3(a) the control gains k_v and c_v acting on the error velocity η are varied in the interval $[0, 2]$ with step 0.14, and the other parameters are kept constant, with $k_p = 1$, $c_p = 1$, $s_F = 1$, and $s_\tau = 1$. In Figure 3(b), the control gains k_p and c_p acting on the hand position error η are varied in the interval $[0, 2]$ with step 0.07, and the other parameters are kept constant, with $k_v = 1$, $c_v = 1$, $s_F = 1$ and $s_\tau = 1$. Our results show how the control gains can be used to modulate the convergence time according to the control specification. Figure 3(c) shows how the stability of the system is challenged by the noise intensity. Indeed, we vary s_F and s_τ in the set $[0, 4]$ with step 0.22, and keep the control gains constant, with $k_v = 1$, $c_v = 1$, $k_p = 1$, and $c_p = 1$. We observe that, as the noise increases, the convergence time becomes higher and higher, up to a certain noise intensity, beyond which the error dynamics become unstable.

VI. Experiments on Ground Robots

A. The experimental arena and the ground robots

The experiments on ground robots were performed at the Research and Engineering Center for Unmanned Vehicles (RECUV) Lab at the University of Colorado Boulder, Boulder CO, USA. A VICON motion tracking system (*VICON Motion Systems, OMG plc (LSE: OMG), Oxford, UK*) was utilized to record the motion of the robots. The VICON marker-based motion capture system at the RECUV lab occupied a volume of $15.24\,\mathrm{m} \times 18.29\,\mathrm{m} \times 6.10\,\mathrm{m}$ (length, width, height) housed in $315.87\ \mathrm{m}^2$ of laboratory space. The system was equipped with 18 VICON Bonita 10 cameras and 6 VICON Vero v2.2 cameras to track each robot identified through five reflective pearl markers (*B&L Engineering, Santa Ana, CA, USA*) positioned on their surface. The cameras were set up to detect reflective markers with diameter as small as $0.005\,\mathrm{m}$, thus allowing the VICON motion tracking system to provide accurate position, velocity, and acceleration data at 100 fps. The motion tracking software further processed the captured frames through discrete Kalman filters to achieve robust 3D-motion estimates, and an external camera (*iPhone 7 Plus, Apple Inc., Cupertino, CA, USA*) was used to record videos for all trials. We emphasize that, although the VICON motion tracking system may provide centralized measurements to all the robots, in view of a decentralized implementation, each robot only used information on their own position and velocity, and on those of their neighbors, according to the decentralized control law (21)-(22). Further, the decentralized control scheme is independently implemented in real time on each robot computer board.

Three robots (*iRobots Create 2, iRobot Corporation, Bedford, MA, USA*), were used in the experiments, see Figure 4(a). Their mass, moment of inertia, and diameter were given in Section V-B. Each robot was customized to house an additional computer board (*Raspberry Pi Foundation, Caldecote, UK*) and a power supply, with the housing units designed in

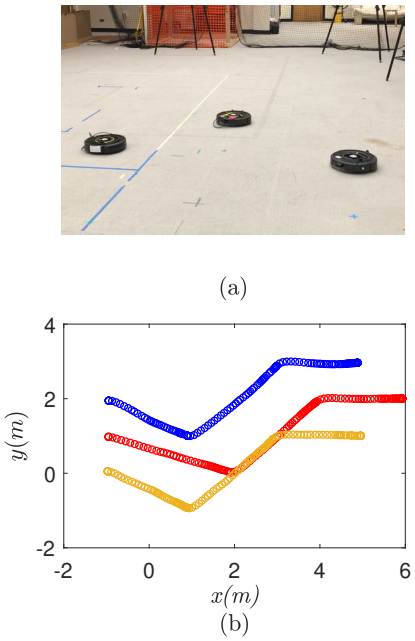

Fig. 4. View of the experimental room with the three robots in formation including the leader identified by a red marker (a) and sample trajectory of the three robots transitioning in between the three predefined goals (b).

Solidworks (*Dassault Systèmes, Waltham, MA, USA*) and manufactured using acrylic sheets and a 3D printer. The computer boards consisted of three *Raspberry Pi*-s operating under Ubuntu and running the Robotic Operating System (ROS, *https://www.ros.org*). Custom code was written using RosPy, a python library for ROS. An open source third party driver "Create Autonomy" downloaded from the github website (*https://github.com/autonomylab/create_autonomy*) was employed to send via serial communication the linear and angular velocity commands to each iRobot Create 2 motherboard. The on-board computers in each robot were programmed to independently issue commands through ROS executing a preprogrammed control scheme.

In the experiments, to recreate real world scenarios where unpredictable uncertainties might affect the robotic system, stochastic noise was introduced to the system actuation following (42)-(46), where $\Delta t = 0.1\text{s}$ corresponds to the rate at wchich the velocity command was sent to the robot actuator and is compatible with the actuation delay. The parameter of the stochastic noise were selected as $s_F = 1$ and $s_\tau = 1$ to reproduce motion on a graveled surface. Further details on the experimental calibration of the noise intensity is reported in the Supplementary Information. In the absence of all terrain robots or exploratory rovers to conduct outdoor experiments or indoor experiments on a surface covered by a granular material, the identified stochastic noise was directly injected into the robot's actuators to avoid damaging the iRobots Create 2 used in the formation control experiments. We emphasize that, in the absence of the control law (21)-(22), the stochastic noise induces unpredictable variations in speed and heading, thus leading to an erratic motion of the robot. Such motion is comparable to what might be observed with all terrain robots or exploratory rovers [78] either moving on an uneven or slippery terrain, having their actuators affected by a fluctuation of the power supply, or their wheels or motor subject to internal or external friction forces.

Although model (7) does not explicitly account for actuation saturation, which is instead observed in practical applications, this is taken into account when setting up our robots, whose speed and turn rate has been capped to the maximum absolute values $0.1\,\text{m}\,\text{s}^{-1}$ and $1\,\text{rad}\,\text{s}^{-1}$, respectively.

B. Experimental validation

The three robots, coupled through a ring network, had to visit the following sequence of three locations:

$$\mathcal{H}_1 = \left\{ \begin{pmatrix} 2 \\ 0 \end{pmatrix}, \begin{pmatrix} 1 \\ 1 \end{pmatrix}, \begin{pmatrix} 1 \\ -1 \end{pmatrix} \right\}, \mathcal{H}_2 = \left\{ \begin{pmatrix} 4 \\ 2 \end{pmatrix}, \begin{pmatrix} 3 \\ 3 \end{pmatrix}, \begin{pmatrix} 3 \\ 1 \end{pmatrix} \right\},$$

$$\mathcal{H}_3 = \left\{ \begin{pmatrix} 6 \\ 2 \end{pmatrix}, \begin{pmatrix} 5 \\ 3 \end{pmatrix}, \begin{pmatrix} 5 \\ 1 \end{pmatrix} \right\},$$

where the first element of each location identifies the desired location for the leader, which, w.l.o.g is labeled as the first node. Initially, the robots were manually positioned at

$$\mathcal{H}_0 = \left\{ \begin{pmatrix} -1 \\ 1 \end{pmatrix}, \begin{pmatrix} -1 \\ 2 \end{pmatrix}, \begin{pmatrix} -1 \\ 0 \end{pmatrix} \right\}.$$

The formation stabilization objective was considered to be achieved when the error value $e_l(t)$ was less than $0.13\,\text{mm}^2$, which corresponds to the estimated mean square error of the motion tracking system. When the i-th location was reached, the robots were automatically assigned the next location to be achieved. Figure 4(b) presents a sample experimental trajectory of the three robots evolving over the three formation objectives. The trajectories illustrate that our control strategy is capable of driving the three robots from their initial position towards the desired sequence of locations. The effectiveness of our approach is also demonstrated through a video of an exemplary experiment provided in the Supplementary Information.

VII. Conclusions

In this work, we tackled the formation control problem for a group of mobile robots modeled as stochastic nonholonomic unicycles. Specifically, we modeled the possible perturbations to the nominal input forces and torques, which may be due to both internal and environmental factors, as stochastic noise acting on the speed and torque dynamics. Then, we designed a decentralized leader-follower control strategy to drive the formation towards a sequence of desired location. Under suitable assumptions on the individual dynamics, the noise intensity, and the graph connecting the robots, we proved that the designed controller can drive almost surely the network towards the desired formation. Then, extensive numerical simulations illustrated how the control gains can be used to counterbalance the noise intensity and regulate the convergence time towards the desired formation. The feasibility of the proposed control strategy was then confirmed through its implementation on a group of ground robots.

The promising results presented in this work suggest that leader-follower decentralized control schemes are a viable approach to formation control of swarms of robots even in the presence of stochastic perturbations to the input forces and torques. When leaders cannot be deployed, the control law should be complemented by an estimation strategy that only relies on the agents' local coordinate systems, see for instance [79]. Future research will be devoted to investigate the robustness to possible failures of the links in the topology connecting the robots, which may add additional uncertainty on the information flow among the robots.

Acknowledgments

The authors wish to thank Eoin Doherty and Branden Adams for helping the setup of the robots.

Author Contributions

V.M., P.D., and S.H. designed the study, V.M., and P.D. performed the analysis, V.M. conducted the experiments on ground robots, and V.M., P.D., and S.H. wrote the manuscript.

References

[1] B. L. Partridge, "The structure and function of fish schools," *Scientific American*, vol. 246, no. 6, pp. 114–123, 1982.

[2] M. Ballerini, N. Cabibbo, R. Candelier, A. Cavagna, E. Cisbani, I. Giardina, V. Lecomte, A. Orlandi, G. Parisi, A. Procaccini *et al.*, "Interaction ruling animal collective behavior depends on topological rather than metric distance: Evidence from a field study," *Proceedings of the National Academy of Sciences*, vol. 105, no. 4, pp. 1232–1237, 2008.

[3] I. Giardina, "Collective behavior in animal groups: theoretical models and empirical studies." *HFSP Journal*, vol. 2, no. 4, pp. 205–19, 2008.

[4] P. Lévy, *Collective intelligence: mankind's emerging world in cyberspace*. Cambridge, MA, USA: Perseus Books, 1997.

[5] D. J. Watts and S. H. Strogatz, "Collective dynamics of 'small-world' networks," *Nature*, vol. 393, no. 6684, pp. 440–442, 1998.

[6] E. Bonabeau, M. Dorigo, D. d. R. D. F. Marco, G. Theraulaz, G. Théraulaz *et al.*, *Swarm intelligence: from natural to artificial systems*. Oxford University Press, 1999, no. 1.

[7] S. Camazine, *Self-organization in Biological Systems*. Princeton, NJ: Princeton University Press, 2003.

[8] D. Karaboga and B. Basturk, "On the performance of artificial bee colony (ABC) algorithm," *Applied Soft Computing*, vol. 8, no. 1, pp. 687–697, 2008.

[9] J. Kennedy, "Swarm intelligence," in *Handbook of nature-inspired and innovative computing*. Springer, 2006, pp. 187–219.

[10] S.-J. Chung, A. A. Paranjape, P. Dames, S. Shen, and V. Kumar, "A survey on aerial swarm robotics," *IEEE Transactions on Robotics*, vol. 34, no. 4, pp. 837–855, 2018.

[11] M. Brambilla, E. Ferrante, M. Birattari, and M. Dorigo, "Swarm robotics: a review from the swarm engineering perspective," *Swarm Intelligence*, vol. 7, no. 1, pp. 1–41, 2013.

[12] P. Arena, L. Fortuna, M. Frasca, and G. Sicurella, "An adaptive, self-organizing dynamical system for hierarchical control of bio-inspired locomotion," *IEEE Transactions on Systems, Man, and Cybernetics, Part B (Cybernetics)*, vol. 34, no. 4, pp. 1823–1837, 2004.

[13] Y. U. Cao, A. S. Fukunaga, and A. Kahng, "Cooperative mobile robotics: Antecedents and directions," *Autonomous Robots*, vol. 4, no. 1, pp. 7–27, 1997.

[14] E. Şahin, "Swarm robotics: From sources of inspiration to domains of application," in *International Workshop on Swarm Robotics*. Springer, 2004, pp. 10–20.

[15] D. Floreano and R. J. Wood, "Science, technology and the future of small autonomous drones," *Nature*, vol. 521, no. 7553, p. 460, 2015.

[16] A. R. Oh, H.and Shirazi, C. Sun, and Y. Jin, "Bio-inspired self-organising multi-robot pattern formation: A review," *Robotics and Autonomous Systems*, vol. 91, pp. 83–100, 2017.

[17] Y. Q. Chen and Z. Wang, "Formation control: a review and a new consideration," in *2005 IEEE/RSJ International Conference on Intelligent Robots and Systems*. IEEE, 2005, pp. 3181–3186.

[18] K.-K. Oh, M.-C. Park, and H.-S. Ahn, "A survey of multi-agent formation control," *Automatica*, vol. 53, pp. 424–440, 2015.

[19] E. Montijano, E. Cristofalo, D. Zhou, M. Schwager, and C. Sagüés, "Vision-based distributed formation control without an external positioning system," *IEEE Transactions on Robotics*, vol. 32, no. 2, pp. 339–351, 2016.

[20] Y. Liu, J. M. Montenbruck, D. Zelazo, M. Odelga, S. Rajappa, H. H. Bülthoff, F. Allgöwer, and A. Zell, "A distributed control approach to formation balancing and maneuvering of multiple multirotor uavs," *IEEE Transactions on Robotics*, vol. 34, no. 4, pp. 870–882, 2018.

[21] W. Qiao and R. Sipahi, "Consensus control under communication delay in a three-robot system: Design and experiments," *IEEE Transactions on Control Systems Technology*, vol. 24, no. 2, pp. 687–694, 2015.

[22] T. Luettel, M. Himmelsbach, and H.-J. Wuensche, "Autonomous ground vehicles – concepts and a path to the future," *Proceedings of the IEEE*, vol. 100, no. Special Centennial Issue, pp. 1831–1839, 2012.

[23] M. Senanayake, I. Senthooran, J. C. Barca, H. Chung, J. Kamruzzaman, and M. Murshed, "Search and tracking algorithms for swarms of robots: A survey," *Robotics and Autonomous Systems*, vol. 75, no. B, pp. 422–434, 2016.

[24] J. Yuh, "Design and control of autonomous underwater robots: A survey," *Autonomous Robots*, vol. 8, no. 1, pp. 7–24, 2000.

[25] N. Bayat, B.and Crasta, A. M. Crespi, A.and Pascoal, and A. Ijspeert, "Environmental monitoring using autonomous vehicles: a survey of recent searching techniques," *Current Opinion in Biotechnology*, vol. 45, pp. 76–84, 2017.

[26] P. DeLellis, F. Garofalo, F. Lo Iudice, and G. Mancini, "State estimation of heterogeneous oscillators by means of proximity measurements," *Automatica*, vol. 51, pp. 378–384, 2015.

[27] F. Lo Iudice, J. A. Acosta, F. Garofalo, and P. DeLellis, "Estimation and control of oscillators through short-range noisy proximity measurements," *Automatica*, 2019, provisionally accepted.

[28] L. Fortuna, M. Frasca, and A. Rizzo, "Chaotic pulse position modulation to improve the efficiency of sonar sensors," *IEEE Transactions on Instrumentation and Measurement*, vol. 52, no. 6, pp. 1809–1814, 2003.

[29] I. D. Couzin, J. Krause, N. R. Franks, and S. A. Levin, "Effective leadership and decision-making in animal groups on the move," *Nature*, vol. 433, no. 7025, pp. 513–516, 2005.

[30] V. Mwaffo, S. Butail, and M. Porfiri, "Analysis of pairwise interactions in a maximum likelihood sense to identify leaders in a group," *Frontiers in Robotics and AI*, vol. 4, p. 35, 2017.

[31] F. Cucker and C. Huepe, "Flocking with informed agents," *Mathematics in Action*, vol. 1, no. 1, pp. 1–25, 2008.

[32] X. Su, H.and Wang and Z. Lin, "Flocking of multi-agents with a virtual leader," *IEEE Transactions on Automatic Control*, vol. 54, no. 2, pp. 293–307, 2009.

[33] V. Mwaffo and M. Porfiri, "Linear analysis of the vectorial network model in the presence of leaders," *Automatica*, vol. 58, pp. 160–166, 2015.

[34] N. Abaid and M. Porfiri, "Leader–follower consensus over numerosity-constrained random networks," *Automatica*, vol. 48, no. 8, pp. 1845–1851, 2012.

[35] S. Zhao, "Affine formation maneuver control of multiagent systems," *IEEE Transactions on Automatic Control*, vol. 63, no. 12, pp. 4140–4155, 2018.

[36] J. Chen, D. Sun, J. Yang, and H. Chen, "Leader-follower formation control of multiple non-holonomic mobile robots incorporating a receding-horizon scheme," *The International Journal of Robotics Research*, vol. 29, no. 6, pp. 727–747, 2010.

[37] R. T. Lawton, R. W. Beard, and B. J. Young, "A decentralized approach to formation maneuvers," *IEEE Transactions on Robotics and Automation*, vol. 19, no. 6, pp. 933–941, 2003.

[38] L. Consolini, F. Morbidi, D. Prattichizzo, and M. Tosques, "Leader–follower formation control of nonholonomic mobile robots with input constraints," *Automatica*, vol. 44, no. 5, pp. 1343–1349, 2008.

[39] C. K. Verginis, A. Nikou, and D. V. Dimarogonas, "Position and orientation based formation control of multiple rigid bodies with collision avoidance and connectivity maintenance," in *2017 IEEE 56th Annual Conference on Decision and Control (CDC)*. IEEE, 2017, pp. 411–416.

[40] ——, "Robust formation control in $\mathbb{SE}(3)$ for tree-graph structures with prescribed transient and steady state performance," *Automatica*, vol. 103, pp. 538–548, 2019.

[41] V. Gazi and B. Fidan, "Coordination and control of multi-agent dynamic systems: Models and approaches," in *International Workshop on Swarm Robotics*. Springer, 2006, pp. 71–102.

[42] S. Mastellone, D. M. Stipanović, C. R. Graunke, K. A. Intlekofer, and M. W. Spong, "Formation control and collision avoidance for multi-agent non-holonomic systems: Theory and experiments," *The International Journal of Robotics Research*, vol. 27, no. 1, pp. 107–126, 2008.

[43] X. Yu and L. Liu, "Distributed circular formation control of ring-networked nonholonomic vehicles," *Automatica*, vol. 68, pp. 92–99, 2016.

[44] A. Pierson and M. Schwager, "Controlling noncooperative herds with robotic herders," *IEEE Transactions on Robotics*, vol. 34, no. 2, pp. 517–525, 2017.

[45] X. Liang, H. Wang, Y.-H. Liu, W. Chen, and T. Liu, "Formation control of nonholonomic mobile robots without position and velocity measurements," *IEEE Transactions on Robotics*, vol. 34, no. 2, pp. 434–446, 2018.

[46] B. Siciliano and O. Khatib, *Springer Handbook of Robotics*. Springer, 2016.

[47] R. P. Anderson and D. Milutinović, "A stochastic optimal enhancement of feedback control for unicycle formations," in *Distributed Autonomous Robotic Systems*. Springer, 2014, pp. 261–274.

[48] L. Jetto, S. Longhi, and G. Venturini, "Development and experimental validation of an adaptive extended kalman filter for the localization of mobile robots," *IEEE transactions on Robotics and Automation*, vol. 15, no. 2, pp. 219–229, 1999.

[49] D. A. B. Lombana, G. Russo, and M. di Bernardo, "Pinning controllability of complex network systems with noise," *IEEE Transactions on Control of Network Systems*, 2018.

[50] M. Annunziato and A. Borzì, "A Fokker–Planck control framework for multidimensional stochastic processes," *Journal of Computational and Applied Mathematics*, vol. 237, no. 1, pp. 487–507, 2013.

[51] S. K. Shah and H. G. Tanner, "Control of stochastic unicycle-type robots," in *2015 IEEE International Conference on Robotics and Automation (ICRA)*. IEEE, 2015, pp. 389–394.

[52] M. S. S. Satoh, H. J. Kappen, "An iterative method for nonlinear stochastic optimal control based on path integrals," *IEEE Transactions on Automatic Control*, vol. 62, no. 1, pp. 262–276, 2017.

[53] B. van der Broek, W. Wiegerinck, and B. Kappen, "Stochastic optimal control of state constrained systems," *International Journal of Control*, vol. 84, no. 3, pp. 597–615, 2011.

[54] V. Gómez, S. Thijssen, A. Symington, S. Hailes, and H. J. Kappen, "Real-time stochastic optimal control for multi-agent quadrotor systems," in *Proceedings of the Twenty-Sixth International Conference on Automated Planning and Scheduling (ICAPS 2016)*, 2016, pp. 468–476.

[55] T. Hida, *Brownian motion*, ser. Applications of Mathematics. New York, NY: Springer, 1980, vol. 11, ch. Brownian motion.

[56] L. Arnold, *Stochastic Differential Equations*. New York, NY: Wiley, 1972.

[57] A. Friedman, *Stochastic differential equations and their applications*. New York, NY: Academic Press, 1976, vol. 2.

[58] X. Mao, "Stochastic versions of the Lasalle theorem," *Journal of Differential Equations*, vol. 153, no. 1, pp. 175–195, 1999.

[59] ——, *Stochastic differential equations and applications*. Chichester, UK: Horwood Publishing Limited, 2007.

[60] C. D. Godsil and G. F. Royle, *Algebraic graph theory*. New York: Springer, 2001.

[61] L. F. R. Turci, P. DeLellis, E. E. N. Macau, M. Di Bernardo, and M. M. R. Simões, "Adaptive pinning control: A review of the fully decentralized strategy and its extensions," *European Physical Journal Special Topics*, vol. 223, no. 13, pp. 2649–2664, 2014.

[62] M. Gitterman, "Harmonic oscillator with fluctuating damping parameter," *Physical Review E*, vol. 69, no. 4, p. 041101, 2004.

[63] V. Seshadri, B. J. West, and K. Lindenberg, "Stability properties of nonlinear systems with fluctuating parameters: I. nonlinear oscillators," *Physica A: Statistical Mechanics and its Applications*, vol. 107, no. 2, pp. 219–240, 1981.

[64] W. Ren and R. W. Beard, *Consensus in Multi-Vehicle Cooperative Control: Theory and Applications*. New York, NY: Springer, 2008.

[65] X. Cai and M. de Queiroz, "Adaptive rigidity-based formation control for multirobotic vehicles with dynamics," *IEEE Transactions on Control Systems Technology*, vol. 23, no. 1, pp. 389–396, 2015.

[66] Z. Sun and Y. Xia, "Receding horizon tracking control of unicycle-type robots based on virtual structure," *International Journal of Robust and Nonlinear Control*, vol. 26, no. 17, pp. 3900–3918, 2016.

[67] W. Jiang, G. Wen, Z. Peng, T. Huang, and A. Rahmani, "Fully distributed formation-containment control of heterogeneous linear multi-agent systems," *IEEE Transactions on Automatic Control*, 2019.
[68] T. Han, Z.-H. Guan, R.-Q. Liao, J. Chen, M. Chi, and D.-X. He, "Distributed finite-time formation tracking control of multi-agent systems via FTSMC approach," *IET Control Theory & Applications*, vol. 11, no. 15, pp. 2585–2590, 2017.
[69] B. Siciliano, L. Sciavicco, L. Villani, and G. Oriolo, *Robotics: modelling, planning, and control*. London, UK: Springer-Verlag, 2010.
[70] D. Liuzza and P. De Lellis, "Pinning control of higher order nonlinear network systems," *IEEE Control Systems Letters*, vol. 5, no. 4, pp. 1225–1230, 2021.
[71] A. Di Meglio, P. De Lellis, and M. di Bernardo, "Decentralized gain adaptation for optimal pinning controllability of complex networks," *IEEE Control Systems Letters*, vol. 4, no. 1, pp. 253–258, 2019.
[72] L. M. Chen, C.-J. Li, J. Mei, and G.-F. Ma, "Adaptive cooperative formation-containment control for networked Euler-Lagrange systems without using relative velocity information," *IET Control Theory & Applications*, vol. 11, no. 9, pp. 1450–1458, 2017.
[73] P. DeLellis, F. Garofalo, and F. Lo Iudice, "The partial pinning control strategy for large complex networks," *Automatica*, vol. 89, pp. 111–116, 2019.
[74] R. Mikulevičius and E. Platen, "Time discrete Taylor approximations for Itô processes with jump component," *Mathematische Nachrichten*, vol. 138, no. 1, pp. 93–104, 1988.
[75] A. Szimayer and R. Maller, "Testing for mean reversion in processes of Ornstein-Uhlenbeck type," *Statistical Inference for Stochastic Processes*, vol. 7, no. 2, pp. 95–113, 2004.
[76] P. E. Kloeden and E. Platen, "A survey of numerical methods for stochastic differential equations," *Stochastic Hydrology and Hydraulics*, vol. 3, pp. 155–178, 1989.
[77] L. Ma and N. Hovakimyan, "Cooperative target tracking in balanced circular formation: Multiple UAVs tracking a ground vehicle," in *Proceedings of the 2013 American Control Conference*, 2013, pp. 5386–5391.
[78] G. Ishigami, G. Kewlani, and K. Iagnemma, "Statistical mobility prediction for planetary surface exploration rovers in uncertain terrain," in *2010 IEEE International Conference on Robotics and Automation*. IEEE, 2010, pp. 588–593.
[79] Q. Yang, M. Cao, H. Garcia de Marina, H. Fang, and J. Chen, "Distributed formation tracking using local coordinate systems," *Systems & Control Letters*, vol. 111, pp. 70–78, 2018.

Violet Mwaffo received the Ph.D. degree in Mechanical Engineering from New York University School of Engineering in 2017. His doctoral research, supported by the National Science Foundation, has focused on data-driven modeling and analysis of collective behavior observed in biological groups. His post-doctoral preparation, supported by the Chancellor Fellowship of the University of Colorado, has explored recent advances in theoretical and experimental study of multi-robotic systems. He was awarded a National Science Foundation GK-12 fellowship in the Applying Mechatronics to Promote Science and Engineering in 2012, a MITSUI-USA foundation fellowship in 2015, and the Chancellor Post-Doctoral Fellowship of the University of Colorado Boulder in 2017. He is currently an Assistant Professor in the Weapons, Robotics and Control Engineering Department at the United States Naval Academy. His research interests include bio-inspired systems, autonomous distributed systems, and artificial intelligence. Dr. Mwaffo serves as a reviewer for several scientific journals and conferences.

Pietro De Lellis (M'14) received the Ph.D. degree in automation engineering from the University of Naples Federico II, Italy, in 2009, where he is currently an Associate Professor of Automatic Control. As a visiting Ph.D. student, in 2009 he spent six months at the NYU Tandon School of Engineering, where he was later appointed Postdoctoral Fellow and Visiting Professor. From 2010 to 2014, he was Adjunct Professor with Accademia Aeronautica (the Italian equivalent of the Air Force Institute of Technology), Pozzuoli, Italy. In 2020, he obtained the National Habilitation as Full Professor. He has authored more than 75 scientific publications that, according to Google Scholar (October 2020), received over 1800 citations. His research interests include analysis, synchronization, and control of complex networks, collective behavior analysis, formation control, decentralized estimation, and evolving financial networks. Dr. De Lellis serves on the editorial board of several international scientific journals and conferences.

Sean Humbert is the Denver Business Challenge Endowed Professor and Associate Chair in the Department of Mechanical Engineering at the University of Colorado, Boulder. He received his B.S. in Mechanical Engineering from the University of California Davis and his M.S. and Ph.D. degrees from Caltech. His fundamental training is in control and dynamical systems, and his main research focus is perception, reduction and feedback principles in biology. His laboratory works with biologists to apply control- and information-theoretic tools to formalize these principles in small animals such as insects, providing insight into the biology and resulting in novel, robust and computationally efficient solutions for engineered systems. Dr. Humbert is a core member of the Board on Army RDT&E, Systems Acquisition and Logistics (BARSL) and is an AIAA Associate Fellow. He is the recipient of the AIAA National Capital Section Hal Andrews Young Scientist/Engineer Award and an ARO Young Investigator Award.